Calorimetric dissection of thermal unfolding of OspA, a predominantly β-sheet protein containing a single-layer β-sheet

ARTICLE *in* JOURNAL OF MOLECULAR BIOLOGY · DECEMBER 2002

Impact Factor: 4.33 · DOI: 10.1016/S0022-2836(02)00974-9 · Source: PubMed

6 AUTHORS, INCLUDING:

Akiko Koide
University of Chicago
65 PUBLICATIONS **2,198** CITATIONS
SEE PROFILE

Shohei Koide
University of Chicago
118 PUBLICATIONS **3,930** CITATIONS
SEE PROFILE

doi:10.1016/S0022-2836(02)00974-9 available online at http://www.idealibrary.com on IDEAL® J. Mol. Biol. (2002) 323, 751–762

JMB

Calorimetric dissection of thermal unfolding of OspA, a predominantly β-sheet protein containing a single-layer β-sheet

Tomoko Nakagawa[1], Hirotaka Shimizu[1], Karl Link[2], Akiko Koide[2] Shohei Koide[2] and Atsuo Tamura[1,3]*

[1]*Graduate School of Science and Technology, Kobe University Nadaku, Kobe 657-8501, Japan*

[2]*Department of Biochemistry and Biophysics, University of Rochester Medical Center, 601 Elmwood Avenue, Box 712 Rochester, NY 14642, USA*

[3]*PRESTO, JST, Japan*

*Corresponding author

Outer surface protein A (OspA) from *Borrelia burgdorferi* is a predominantly β-sheet protein comprised of β-strands β1–β21 and a short C-terminal α-helix. It contains two globular domains (N and C-terminal domains) and a unique single-layer β-sheet (central β-sheet) that connects the two domains. OspA contains an unusually large number of charged amino acid residues. To understand the mechanism of stabilization of this unique β-sheet protein, thorough thermodynamic investigations of OspA and its truncated mutant lacking a part of the C-terminal domain were conducted using calorimetry and circular dichroism. The stability of OspA was found to be sensitive to pH and salt concentration. The heat capacity curve clearly consisted of two components, and all the thermodynamic parameters were obtained for each step. The thermodynamic parameters associated with the two transitions are consistent with a previously proposed model, in which the first transition corresponds to the unfolding of the C-terminal domain and the last two β-strands of the central β-sheet, and the second transition corresponds to that of the N-terminal domain and the first β-strand of the central β-sheet in the second peak. The ratio of calorimetric and van't Hoff enthalpies indicates that the first peak includes another thermodynamic intermediate state. Large heat capacity changes were observed for both transitions, indicative of large changes in the exposure of hydrophobic surfaces associated with the transitions. This observation demonstrates that hydrophobic parts are buried efficiently in the native structure in spite of the low content of hydrophobic residues in OspA. By decomposing the enthalpy, entropy, and Gibbs free energy into contributions from different interactions, we found that the enthalpy changes for hydrogen bonding and polar interactions are exceptionally large, indicating that OspA maintains its stability by making full use of its unique β-sheet and high content of polar residues. These thermodynamic analyses demonstrated that it is possible to maintain protein tertiary structure by making effective use of an unusual amino acid composition.

Keywords: calorimetry; β-sheet; OspA; thermodynamics; hydration

Introduction

Calorimetric measurement, especially differential scanning calorimetry (DSC), has been the most powerful tool for the investigation of thermal unfolding of proteins,[1] since it is the only method to obtain the true (calorimetric) enthalpy, while other methods, such as spectroscopic measurements, give only the apparent (van't Hoff) enthalpy. Comparison of the calorimetric enthalpy with the van't Hoff enthalpy, which can be

Present address: A. Koide & S. Koide, University of Chicago, Chicago, IL 60637, USA.

Abbreviations used: ASA, accessible surface area; DSC, differential scanning calorimetry; OspA, outer surface protein A.

E-mail address of the corresponding author: atamura@kobe-u.ac.jp

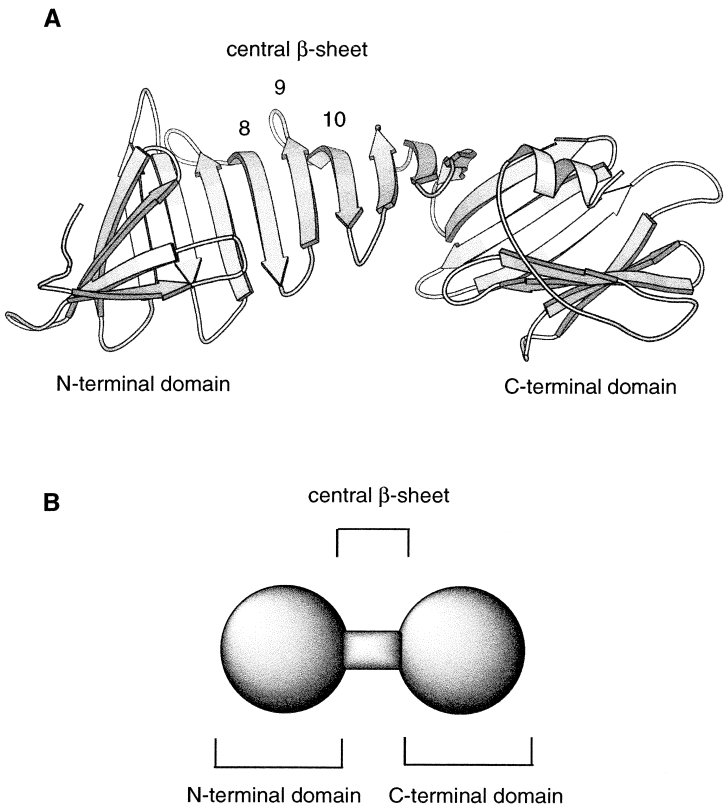

Figure 1. (a) Ribbon model of the OspA crystal structure. (b) A drawing of the OspA structure. It contains a single-layer β-sheet termed the central β-sheet (strand 8–10), which connects the N-terminal domain (N terminus–strand 7) and C-terminal domain (strand 11–C terminus).

obtained simultaneously from one DSC scan, leads to detection of thermodynamic intermediate states. Also, one can derive the change in the heat capacity (ΔC_p) between any two states from a DSC scan. ΔC_p defines the enthalpy, entropy, and free energy at any temperature and thus is regarded as the most important thermodynamic parameter. In view of the structure–thermodynamics relationship, the heat capacity change as well as the other thermodynamic parameters can be related to the structure of a protein, especially to the interaction of water molecules with the protein. These interactions include hydration of non-polar and polar residues, and hydrogen bonding.[2]

Here, we report a thermodynamic study of a predominantly β-sheet protein, Outer surface protein A (OspA), from the Lyme disease spirochete *Borrelia burgdorferi*. OspA is an abundant 31 kDa immunogenic lipoprotein. It is used as a vaccine against Lyme disease, and very recently its role in the attachment of *Borrelia* to the gut of the tick vector has been implicated.[3,4] The crystal structure of a soluble, non-lipidated form of recombinant OspA (28 kDa) was determined in a complex with the Fab fragment of a mouse monoclonal antibody (Figure 1).[5] OspA consists of 21 consecutive antiparallel β-strands and a C-terminal α-helix. It has a dumbbell-shaped structure in which two globular domains, termed the N-terminal domain (N terminus-β7, residues 18–107) and C-terminal domain (β11-C terminus, residues 143–273), are connected by the central β-sheet (β8–β10, residues 108–142). Note that the boundaries of these three segments are based solely on visual inspection of the OspA structure, and that we do not imply these segments correspond directly to folding and/or functional domains. Nuclear magnetic resonance (NMR) spectroscopy and solution small-angle X-ray-scattering analyses have demonstrated that the solution conformation of OspA in the absence of the bound antibody fragment is close to that of the crystal structure.[6,7] The central, "single-layer" β-sheet is exposed to the solvent on both faces and this segment does not contain a hydrophobic core. Nevertheless, the entire OspA molecule, including the central β-sheet, is very rigid and stable.[8] We found that the single-layer β-sheet buries non-polar surfaces to an extent similar to that found for small globular proteins that do contain a hydrophobic core.[8] The single-layer β-sheet architecture appears to exploit the long aliphatic side-chains of polar amino acid residues, such as Glu and Lys, to achieve effective burial of non-polar surfaces in a manner conceptually analogous to the lipid bilayer, where charged head groups are exposed to the solvent and aliphatic moieties are aligned to form a hydrophobic layer. Furthermore, the central β-sheet can be extended by inserting a β-hairpin unit corresponding to strand 9–turn–strand 10,[9] demonstrating that the single-layer β-sheet is an intrinsically stable structure in the structural context of OspA. The high degree of stability of the single-layer β-sheets is in stark contrast to the low degrees of stability observed for isolated small β-sheets,[10,11] implying the importance of capping the two edges of an isolated β-sheet. In addition, OspA has a large number of charged amino acid residues, with 42

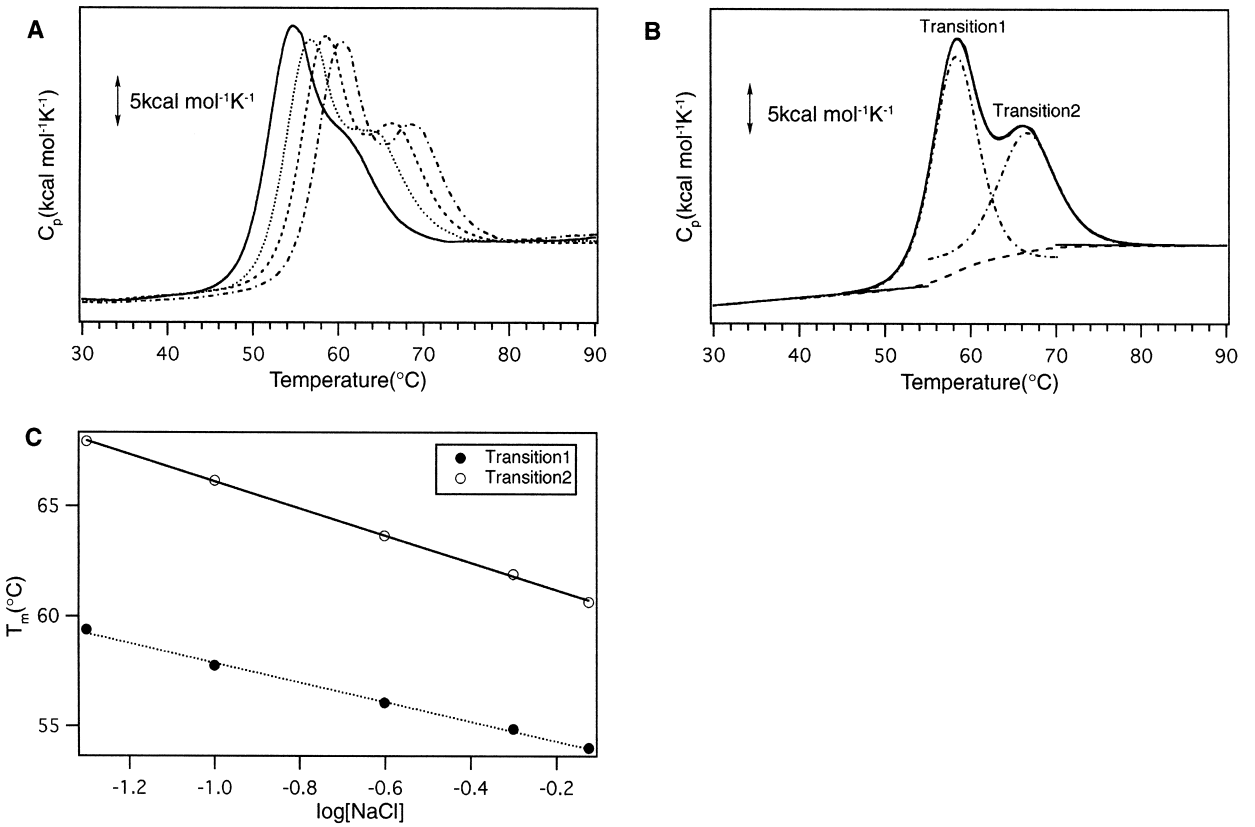

Figure 2. (a) DSC traces of OspA at pH 6 with varying concentrations of NaCl. (50 mM, dot-dashed curve; 100 mM, broken-line curve; 250 mM, dotted curve; 750 mM, continuous curve. (b) DSC trace of OspA at pH 6 with 100 mM NaCl. The peaks with lower and higher melting temperatures are designated Transition1 and Transition2, respectively. The continuous curve is the experimental DSC curve. The two continuous lines show the linearly fit heat capacities for the native (C_{pN}) and denatured (C_{pD}) states. The broken curve shows a calculated baseline. Dot-dashed curves were derived by deconvolution of the original DSC curve. (c) Transition temperatures of the two thermal transitions plotted *versus* log[NaCl]. The filled and open circles indicate the transition temperatures for Transition1 and Transition2, respectively.

Lys, two Arg, 18 Asp, and 23 Glu among a total of 256 residues distributed throughout the whole molecule.[5] Thus, calorimetric studies of OspA should provide new insights into the β-sheet formation and into contributions of electrostatic interactions to protein stability.

It is especially interesting and challenging to find the stabilizing forces of β-sheet, which are predominantly non-local in nature and thus less well understood compared to the local interactions of α-helix formation. So far, only a limited number of β-sheet proteins have been studied thoroughly with calorimetry, e.g. interleukin 1β,[12] the SH3 domain,[13] human acidic fibroblast growth factor,[14] and neocarzinostatin.[15] Among them, unfolding intermediate states were found in only two cases; human acidic fibroblast growth factor and neocarzinostatin. In contrast, intermediates have frequently been found for all-α and for α/β proteins.[1] This difference may be because the interaction maintaining the β-sheet is long-ranged and thus the cooperativity of unfolding is strictly retained, while the local α-helical interaction can prevail in the course of unfolding. In addition, *de novo* design of β-sheet proteins has succeeded in only a limited number of cases,[10,11,16–18] suggesting that the structural principle that governs the β-sheet structure is not understood fully. Therefore, OspA is expected to become a valuable model system to study β-sheet formation. Our preliminary calorimetric study revealed that OspA undergoes a two-step denaturation.[19] NMR identified that the C-terminal globular domain denatured first and the N-terminal domain second. The last two strands of the central β-sheet (β9 and β10) denatured with the C-terminal domain, while the first strand (β8) denatured with the N-terminal domain. In this work, we undertook thorough thermodynamic studies of OspA by means of ultrasensitive DSC and CD spectroscopy to identify the energetic basis of maintaining this unique β-sheet protein.

Results

Ionic effects on thermal unfolding of OspA at neutral pH

DSC measurements were performed at around pH 6 with increasing concentration of NaCl to examine the effect of the ionic strength. We found

Table 1. Thermodynamic parameters for thermal transition of OspA at pH 6 with various concentration of NaCl

NaCl[a]	Conc.[b]	t_{m1}[c]	t_{m2}	ΔC_{pex1}[d]	ΔC_{pex2}	ΔH_{cal1}[e]	$\Delta H_{vH1}/\Delta H_{cal1}$[f]	ΔH_{cal2}	$\Delta H_{vH2}/\Delta H_{cal2}$
50	2.42	59.4	67.9	1.99	1.37	148	0.84	105	0.98
100	2.87	57.8	66.2	2.23	1.31	148	0.74	105	0.97
250	1.07	56.1	63.7	2.50	1.01	145	0.83	98.9	0.98
500	1.31	54.9	61.9	2.13	1.17	147	0.82	97.5	0.97
750	1.93	54.0	60.6	2.66	1.44	155	0.75	93.0	1.01
Mean				2.30 ± 0.27	1.26 ± 0.17		0.80 ± 0.05		0.98 ± 0.02

[a] Concentration of NaCl in mM.
[b] Concentration of OspA in mg ml^{-1}.
[c] Denaturation temperatures in °C.
[d] Heat capacity changes upon protein unfolding in kcal mol^{-1} K^{-1} at t_m of each transition.
[e] Calorimetric enthalpies upon protein unfolding in kcal mol^{-1}.
[f] Ratios between van't Hoff and calorimetric enthalpies.

a dramatic decrease in the transition temperature with increasing concentration of NaCl (Figure 2(a)). This suggests that the native structure of OspA contains a significant number of favorable electrostatic interactions between charged residues, which are weakened by the increasing amount of the salt in the solution.

These DSC curves were analyzed according to a scheme $N \rightleftharpoons I \rightleftharpoons D$,[20] where N, I, and D represent the native, intermediate, and denatured states, respectively. An excellent agreement of the calculated curve with the experimental data (Figure 2(b)) supports this scheme, and shows that the thermal denaturation of OspA at neutral pH proceeds *via* at least one intermediate state. We designate the transition at the lower temperature as Transition1, and the other as Transition2. The heat capacities of the native and denatured states were assumed to be linearly dependent on the temperature (i.e. $C_{pN}(t) = a + bt$ and $C_{pD}(t) = c + dt$ where a, b, c and d are constants), and that of the intermediate state is the weighted average of those for the native and denatured state proportional to the transition enthalpies for the two transitions:

$$C_{pI}(t) = C_{pN}(t) + \{\Delta H_1/(\Delta H_1 + \Delta H_2)\}\{C_{pD}(t) - C_{pN}(t)\} \quad (1)$$

where ΔH_1 and ΔH_2 are the transition enthalpies for Transition1 and Transition2, respectively, and T is the temperature. Deconvolution of the DSC curve into the two components was carried out based on these baselines (Figure 2(b)). The heat capacity changes of N to I (Transition1) and I to D (Transition2) were defined as

$$\Delta C_{pex1} = C_{pI}(t_{m1}) - C_{pN}(t_{m1})$$
$$\Delta C_{pex2} = C_{pD}(t_{m2}) - C_{pI}(t_{m2}) \quad (2)$$

where ΔC_{pex1} and ΔC_{pex2} are the changes in heat capacity upon unfolding, and t_{m1} and t_{m2} are the temperatures at which the transitions are half-completed for Transition1 and Transition2, respectively. Thermodynamic parameters for these transitions are summarized in Table 1. The $\Delta H_{vH}/\Delta H_{cal}$ ratio is nearly equal to unity for Transition2, indicating that the transition is essentially a two-state process between I and D. In contrast, the $\Delta H_{vH}/\Delta H_{cal}$ ratio for Transition1 is significantly lower than unity, indicating that at least another intermediate state exists between N and I. We previously showed that Transition1 corresponds to unfolding of β9–C terminus, while Transition2 corresponds to that of N terminus-β8.[19] Thus, our present results show that β9–C terminus unfolds *via* a thermodynamic intermediate state.

We found that the transition temperatures were related linearly to the logarithm of salt concentration (Figure 2(c)), with the following relationships:

$$t_{m1} = -4.47(\pm 0.14)\log[\mathrm{NaCl}] + 53.4(\pm 0.11)$$
$$t_{m2} = -6.17(\pm 0.09)\log[\mathrm{NaCl}] + 59.9(\pm 0.07) \quad (3)$$

Thus, salt has a larger destabilizing effect for Transition2. We then calculated the number of ions taken up from the buffer during denaturation (Δn) according to the model for specific binding of the ion to the protein.[21] The numbers obtained for Δn were 1.1 and 1.2 for Transition1 and Transition2, respectively, suggesting that about one molecule in total of the ion is affecting the change in stability in total for each step. These numbers, however, can be interpreted either as specific salt binding to a single site or as a collection of weaker effects at multiple sites.

Thermal unfolding at acidic pH

We then characterized the thermal unfolding of OspA at acidic pH. In order to obtain thermodynamic parameters accurately, it is necessary to perturb the stability of a protein in a wide temperature range. We found that lowering pH from 3.82 to 3.21 resulted in significant changes in stability of OspA (Figure 3(a) and (b)), which are sufficient to obtain precise thermodynamic parameters. More DSC experiments were carried out at a pH range between 3.82 and

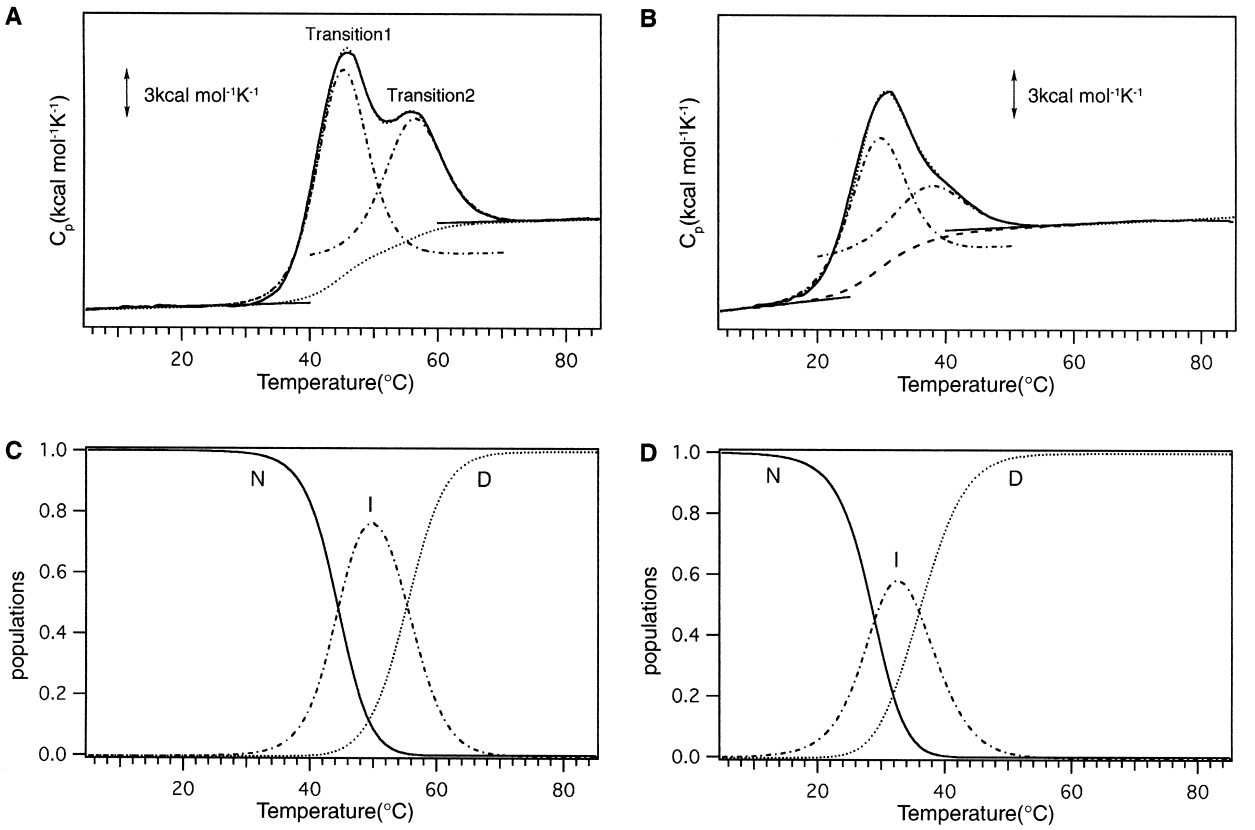

Figure 3. DSC trace of OspA at (a) pH 3.82 and (b) at pH 3.21. (c) Temperature-dependence of the populations of the native (N, continuous curve), intermediate (I, dot-and-dash curve), and denatured (D, dotted curve) states at pH 3.82. (d) Temperature-dependence of each population at pH 3.21.

3.21 (Table 2). OspA aggregated in more acidic solution, rendering DSC measurements impossible. The DSC curves fit well with the two-step scheme, $N \rightleftharpoons I \rightleftharpoons D$, indicating that the thermal denaturation of OspA at the acidic pH proceeds *via* at least one intermediate state (Table 2). The populations of the three species including the intermediate state were calculated and are shown in Figure 3(c) and (d).

The transition temperatures were found to be correlated linearly with pH (Figure 4(a)) with the following relationships:

$$t_{m1} = 25.1(\pm 2.0)\ \mathrm{pH} - 50.6(\pm 7.0)$$
$$t_{m2} = 31.1(\pm 2.0)\mathrm{pH} - 62.5(\pm 6.7) \quad (4)$$

These slopes are within the range of reported values for other proteins of similar size, such as 33.9 (°C pH^{-1}) for *Streptomyces subtilisin* inhibitor (23 kDa).[20] The greater dependence of t_m on pH for Transition2 coincides with larger destabilizing

Table 2. Thermodynamic parameters for thermal transition of OspA at various pH

pH	Conc.	t_{m1}	t_{m2}	ΔH_{cal1}	ΔH_{cal2}	Δv_1[a]	Δv_2	ΔC_{pex1}	ΔC_{pex2}
3.20	1.79	28.7	36.1	99.7	44.8	3.77	3.62	3.55	1.40
3.21	2.31	28.5	35.8	96.1	50.6	3.70	3.49	2.44	1.22
3.27	1.52	31.8	39.6	95.6	51.4	4.22	3.89	2.86	1.37
3.35	1.20	35.3	43.3	110	63.8	4.44	4.11	2.50	1.49
3.36	2.02	34.2	42.6	105	70.7	3.96	3.66	2.37	1.39
3.46	1.24	37.6	46.0	104	73.5	4.56	4.11	2.20	1.31
3.52	2.20	38.7	48.3	108	80.9	4.26	4.36	1.96	1.34
3.67	2.04	41.1	51.5	132	85.1	3.95	4.16	2.84	1.80
3.82	2.19	44.4	55.2	134	89.2	4.15	4.38	2.81	1.87
6.00	2.42	59.4	67.9	148	105			1.99	1.37
6.33	1.86	59.9	68.5	157	104			2.23	1.48
Mean						4.11 ± 0.29	3.98 ± 0.32	2.52 ± 0.47	1.46 ± 0.20

[a] The number of protons taken up from the buffer upon protein unfolding. Other parameters are described in Table 1.

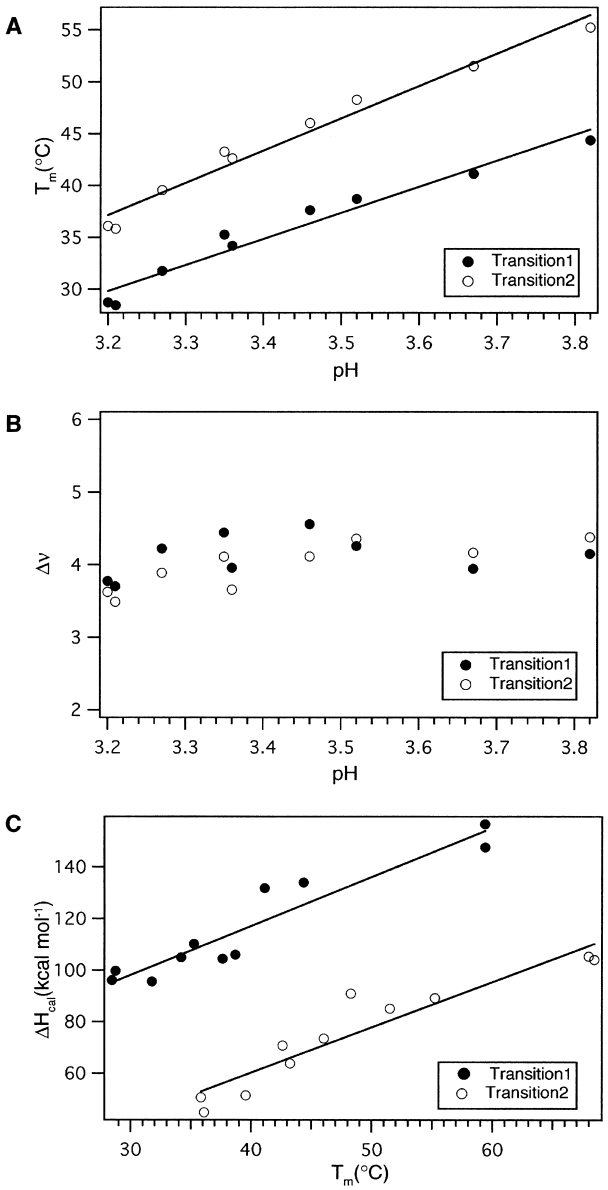

Figure 4. (a) The transition temperatures of OspA denaturation plotted versus pH. The closed and open circles indicate the transition temperatures for Transition1 and Transition2, respectively. (b) The number of protons taken up from the buffer by the protein upon thermal transition, Δν, plotted *versus* pH. (c) Calorimetric enthalpies in the presence of 50 mM NaCl plotted *versus* transition temperatures, t_m.

effect on salt concentration observed for Transition2 (Figure 2(c)).

From the slopes in equation (4), we determined the number of protons taken up from the buffer in denaturation according to the following equation derived from the van't Hoff equation:

$$\Delta\nu = (1000\Delta H(t_m)/2.303Rt_{m2})(dt_m/dpH) \quad (5)$$

The Δν values for both Transition1 ($\Delta\nu_1$) and Transition2 ($\Delta\nu_2$) lie around 4 (Figure 4(b)), suggesting that four acidic residues, Asp and/or Glu that have anomalous pK_a values in the native state, are contributing to the pH-dependence of thermal stability for each transition. The sum of $\Delta\nu_1$ and $\Delta\nu_2$ is about 8, which is higher than reported Δν values for other proteins, e.g. 6 for SSI[20] and 1 for an all-β-protein, cold-shock protein (Csp; 7.5 kDa).[22] This may reflect the unusually high content of charged amino acid residues (85 out of 257 residues) in OspA.

ΔC_p derived from temperature-dependence of ΔH_{cal}

We then obtained the heat capacity change from the slope of enthalpies against temperature, according to the following equation:

$$\Delta C_{pslope} = (\delta\Delta H/\delta t)_p \quad (6)$$

All the transition enthalpies obtained from DSC experiments were plotted as a function of the transition temperatures (Figure 4(c)). Since there is no His in OspA, it is not necessary to correct for the heat of ionization of His, which is usually not negligible when comparing the acidic data with neutral data.[23] Heat of ionization of acidic residues is negligible in the glycine buffer used in this study,[1] and thus the experimental enthalpy is regarded as originating from the protein itself. From the slope, we obtained ΔC_{pslope} for Transition1 as 1.90(±0.21) kcal mol^{-1} K^{-1}, and that for Transition2 as 1.76(±0.21) kcal mol^{-1} K^{-1} (1 cal = 4.184 J). These numbers are in a fairly good agreement with ΔC_{pex} (Table 2).

Table 3. Thermodynamic parameters for thermal transition of OspA and OspA[27–163] at pH 6

Protein	Method	pH	t_{m1}	t_{m2}	ΔH_{cal1}	ΔH_{vH1}	$\Delta H_{vH1}/\Delta H_{cal1}$	ΔH_{cal2}	ΔH_{vH2}	$\Delta H_{vH1}/\Delta H_{cal2}$
OspA	DSC	6.00	59.4	67.9	148	124	0.84	105	103	0.98
		6.33	59.8	68.5	157	121	0.77	104	107	1.03
OspA[27–163]	DSC	6.00		66.5				111	93	0.84
		6.29		67.1				102	92	0.91
OspA	Near-UV CD	6.05	58.3			117				
OspA	Far-UV CD	6.33	58.6	66.8		122			110	
OspA[27–163]	Far-UV CD	6.30		68.3					105	

Thermodynamic parameters are described in Table 1.

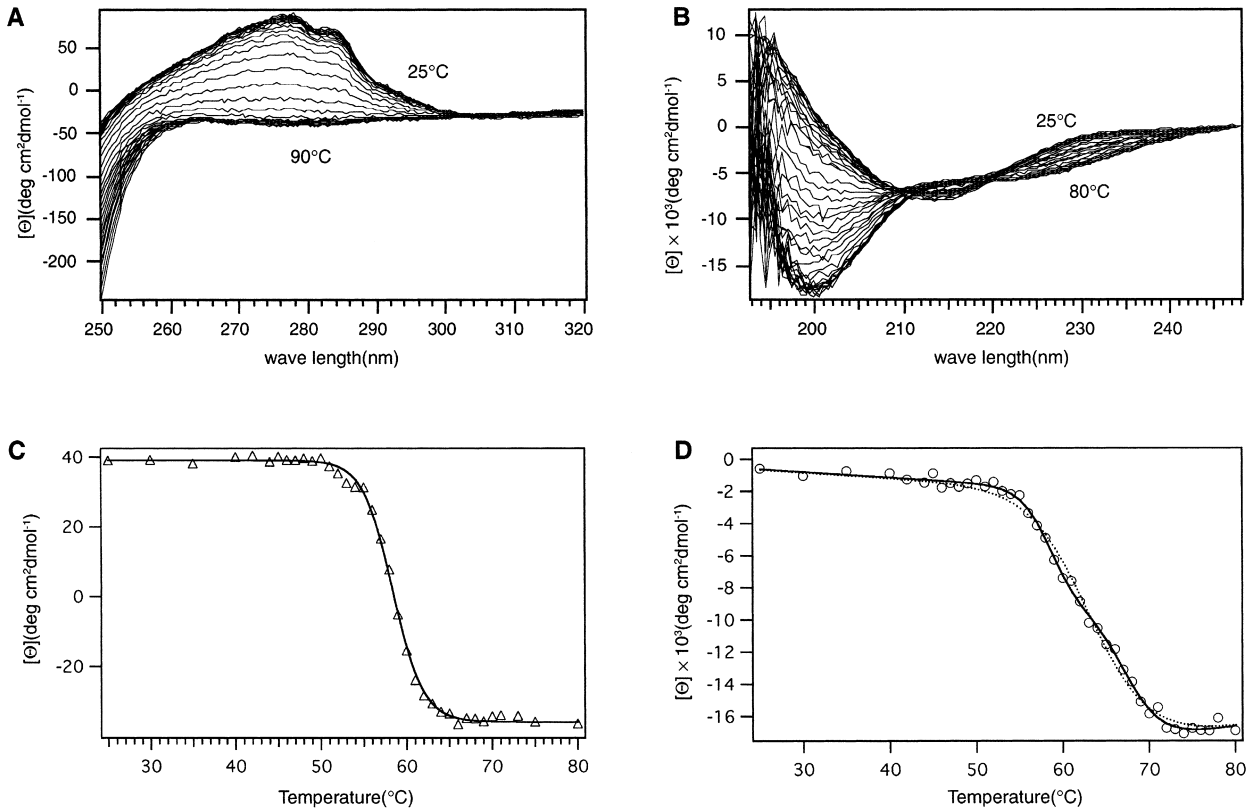

Figure 5. Temperature-dependence of CD spectra of OspA in the (a) near-UV and (b) far-UV regions. The temperature was varied from 25 °C to 90 °C (near-UV) or to 80 °C (far-UV). Plots of ellipticity at (c) 263 nm and (d) 202 nm *versus* temperature. Data were fit with a scheme N ⇌ D for the near-UV region and a scheme N ⇌ I ⇌ D for the far-UV region and the thermodynamic parameters thus obtained are listed in Table 3. In (d), the dotted curve represents the result of curve-fitting according to a scheme N ⇌ D.

Structural transition revealed by circular dichroism spectroscopy

We then characterized the thermal denaturation of OspA using circular dichroism (CD) spectroscopy. In OspA, one Trp residue at position 216 and three Tyr residues at positions 147, 165 and 248 are located in the C-terminal domain, and only one Tyr residue at position 52 is located in the N-terminal domain. Since Trp residues usually dominate the near-UV CD spectrum of a protein containing both Trp and Tyr,[24] the spectral changes in near-UV CD of OspA can be attributed to the conformational changes of the C-terminal domain. The transition temperature obtained from near-UV CD measurements (Figure 5(c)) is in a good agreement with that of Transition1 of OspA determined from calorimetric measurements (Table 3).

The conformational transition of OspA monitored by far-UV CD (Figure 5(b) and (d)) showed a clear difference from that by near-UV CD (Figure 5(a) and (c)). Although a previous report concluded that the transition of OspA monitored by far-UV CD was two-state,[25] more detailed analysis shown here indicates clearly that the experimental data were best fit when an intermediate is assumed (Figure 5(d)). In fact, the standard deviation of the fitting for the far-UV data was improved (273 *versus* 525) when we employed the three-state mechanism rather than the two-state transition (Figure 5(d)). The transition temperature for the first transition is 58.3 °C, which corresponds to the transition temperature obtained from the near-UV CD and that from DSC for Transition1. The second transition temperature is 66.8 °C, which almost agrees with the transition temperature obtained from the DSC measurement for Transition2. It is thus concluded that thermal transition of the far-UV CD spectra includes each of the two major transitions detected by DSC (Transition1 and 2), although Transition1 was not a perfect two-state transition. The denaturation temperature, t_m, and the van't Hoff enthalpies, ΔH_{vH}, obtained by curve fitting are shown in Table 3. These values agree with those obtained from the DSC measurement (Table 3).

In addition, we investigated thermal unfolding of an N-terminal fragment (OspA[27–163]) that corresponds to β-strands 1–12. Our NMR studies have shown that in this N-terminal fragment the region corresponding to β1–β11 is folded but the last, 12th β-strand is disordered.[26] The thermal denaturation of this fragment approximately corresponds to the second transition of the whole OspA protein, confirming our assignments of the two thermal transitions of OspA. The melting curves

Table 4. Comparison of heat capacity of OspA calculated based on ASA ($\Delta C_{p\mathrm{ASA}}$) and that experimentally obtained ($\Delta C_{p\mathrm{ex}}$)

		$\Delta\mathrm{ASA}_{\mathrm{np}}$ [a]	$\Delta\mathrm{ASA}_{\mathrm{p}}$	$\Delta C_{p\mathrm{ASA}}$ [b]	$\Delta C_{p\mathrm{ex}}$
OspA	(1) β-9–C terminus	10,424	7371	2.30	2.52 ± 0.47
	(2) N terminus–β8	6395	4254	1.45	1.46 ± 0.20
OspA[27–163]	N-terminal domain + central β-sheet (27–163):N terminus–β12	9098	6659	1.98	1.44 ± 0.04

[a] Non-polar and polar-accessible surface area changes upon protein unfolding, $\Delta\mathrm{ASA}_{\mathrm{np}}$ and $\Delta\mathrm{ASA}_{\mathrm{p}}$, respectively, in Å. Accessible surface area of OspA are obtained[8] from the PDB coordinate. Non-polar surface corresponds to the surface of all carbon atoms except for amide, carboxylate and guanidino carbons. Exposed surface area was normalized to the total solvent-accessible surface area.[36]

[b] The values of $\Delta C_{p\mathrm{ASA}}$ in kcal mol^{-1} K^{-1} are calculated from equation (7); $\Delta C_{p\mathrm{ASA}} = (0.32 \pm 0.04)(\Delta\mathrm{ASA}_{\mathrm{np}}) - (0.14 \pm 0.04)(\Delta\mathrm{ASA}_{\mathrm{p}})$.

of OspA[27–163] were fitted with a scheme N ⇌ D (data not shown). The transition temperature obtained from far-UV CD region was close to that obtained from DSC measurement (Table 3), suggesting that DSC and CD detect the same structural transition.

Discussion

Relationship between structure and thermodynamics revealed by hydration effect

ΔC_p can be divided into two factors; positive contribution from the exposure of non-polar groups and negative contribution from the exposure of polar groups. Spolar *et al*. determined the following equation to estimate ΔC_p from the change in the non-polar ($\Delta\mathrm{ASA}_{\mathrm{np}}$) and polar ($\Delta\mathrm{ASA}_{\mathrm{p}}$) accessible surface area:[27]

$$\Delta C_{p\mathrm{ASA}} = (0.32 \pm 0.04)(\Delta\mathrm{ASA}_{\mathrm{np}}) - (0.14 \pm 0.04) \times (\Delta\mathrm{ASA}_{\mathrm{p}}) \quad (7)$$

Our previous NMR study showed that the C-terminal folding unit (β9–C terminus) denatured first, followed by the denaturation of the N-terminal folding unit (N terminus-β8).[19] According to equation (7), ΔC_p estimated from ΔASA of β9–C terminus and N terminus-β8 were 2.30 and 1.45 kcal mol^{-1} K^{-1}, respectively, which agree very well with the experimental values, $\Delta C_{p\mathrm{ex}}$ (2.52 and 1.46 kcal mol^{-1} K^{-1}, respectively) (Table 4). This excellent agreement supports our model for OspA thermal unfolding. It is important to note that the $\Delta C_{p\mathrm{ex}}$ values for OspA do not significantly deviate from those predicted solely with ΔASA of non-polar and polar groups. This suggests that the underlying mechanism for stabilizing the unique structure of OspA is not fundamentally different from those for more typical, globular proteins.

We found that ΔC_p calculated from ΔASA of OspA[27–163] (1.98 kcal mol^{-1} K^{-1}) was significantly larger than the experimental value, $\Delta C_{p\mathrm{ex}}$ (1.44 kcal mol^{-1} K^{-1}) (Table 4). Rather, $\Delta C_{p\mathrm{ex}}$ for OspA[27–163] was close to that for Transition2 of OspA (1.46 kcal mol^{-1} K^{-1}), indicating that thermal transition sensitive to ΔC_p corresponds to β1–β8 of OspA[27–163] (Table 4). Thus, it is likely that residues in β9–β12 of OspA[27–163] are accessible to solvent water. However, our previous NMR results[26] demonstrated that β9–β11 retained the secondary structure judging from ^{13}C secondary shift and ^{1}H,^{15}N NOE, although the amide protons in β9–β12 have very little protection (<100) from solvent H–^{2}H exchange. In this fragment, β12 was disordered. Taken together, these data suggest a rather paradoxical state of a folded β-sheet in which amino acid residues are highly accessible to the solvent. A possible explanation of this is that β9–β11 is slowly (micro- to millisecond timescale or slower) fluctuating, while keeping the average secondary structure. If water molecules can penetrate to the interior of this loosely folded β-sheet segment, its structural changes would result in a negligible ΔC_p value, since ΔC_p is determined primarily by water-protein interactions.[28] Detailed structural analysis of this fragment is underway.

Thermodynamic mechanism of OspA unfolding

We then deduce the unfolding mechanism from the calorimetric data and previously obtained structural information. The $\Delta H_{\mathrm{vH}}/\Delta H_{\mathrm{cal}}$ ratio for Transition1 was smaller than unity at pH 6 (Table 3), suggesting that there is an intermediate state in Transition1. What is the nature of this intermediate state? We have shown that in OspA[27–163], N terminus–β11 retains its structure in the absence of the β13–C terminus segment, although β9–β11 appears to have an increased flexibility. Since the

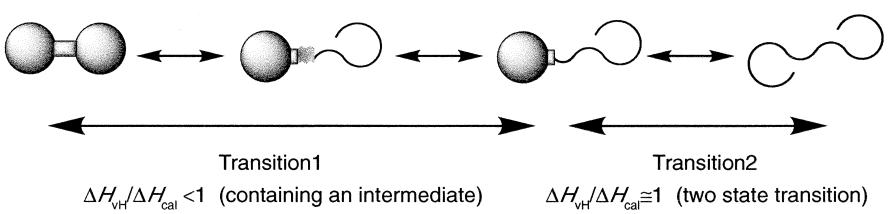

Figure 6. A representation of denaturing mechanisms for OspA.

Table 5. The enthalpy, entropy, and Gibbs energy for unfolding of OspA at 25 °C

	β9–C terminus (Transition1)	N terminus–β8 (Transition2)	Full-length[a]
Enthalpy (kcal mol^{-1})			
ΔH_{cal}[b]	89	34	123
ΔH_{alp}^{hyd}	−282	−179	−460
ΔH_{arm}^{hyd}	−28	−8.4	−36.4
ΔH_{pol}^{hyd}	−2183	−1260	−3443
ΔH^{vdw}	323	195	518
ΔH^{HB}	2258	1286	3544
Δh^{HB}	19	21	20
Entropy (cal mol^{-1} K^{-1})			
ΔS^{exc}	257	85.7	343
ΔS_{alp}^{hyd}	−1330	−850	−2180
ΔS_{arm}^{hyd}	−60.0	−18.1	−78.1
ΔS_{pol}^{hyd}	−1454	−834	−2288
ΔS^{cnf}	3101	1788	4889
Δs^{cnf}	20.0	18.6	19.5
Gibbs energy (kcal mol^{-1})			
ΔG^{exd}	12	8	20
ΔG_{alp}^{hyd}	116	74	190
ΔG_{arm}^{hyd}	−10	−3	−13
ΔG_{pol}^{hyd}	−1749	−1011	−2760
Δg_{hyd}^{HB}	4.4	4.6	4.4

[a] β9–C terminus and N terminus–β8 contain 155 and 96 amino acid residues, respectively.

[b] ΔH_{cal}: the calorimetric enthalpies of protein unfolding at 25 °C extrapolated by using the heat capacity changes, 1.90 kcal mol^{-1} K^{-1} and 1.76 kcal mol^{-1} K^{-1} for β9–C terminus and N terminus–β8, respectively. ΔH_{alp}^{hyd}, ΔH_{arm}^{hyd} and ΔH_{pol}^{hyd}: the enthalpies of hydration of aliphatic, aromatic and polar groups upon protein unfolding, respectively. ΔH^{vdw}: the enthalpy of van der Waals interactions between non-polar groups in protein. ΔH^{HB}: the total enthalpy of internal hydrogen bonding in protein. Δh^{HB}: the enthalpy of an internal hydrogen bond in a protein. The number of hydrogen bonds: 117 and 60 for β9–C terminus and N terminus–β8, respectively.

[c] ΔS^{ex}: the experimentally determined entropy of protein unfolding. ΔS_{alp}^{hyd}, ΔS_{arm}^{hyd} and ΔS_{pol}^{hyd}: the entropies of hydration of aliphatic, aromatic and polar group upon protein unfolding, respectively. ΔS^{cnf}, the configurational entropy of unfreezing of the backbone-chain and of unpacking of the side-chain groups. Δs^{cnf}, the configurational entropy per residue.

[d] ΔG^{ex}: experimental Gibbs energy at pH 6. ΔG_{alp}^{hyd}: ΔG_{arm}^{hyd} and ΔG_{pol}^{hyd}: the Gibbs energy of hydration of aliphatic, aromatic and polar groups upon protein unfolding, respectively. Δg_{hyd}^{HB}: the total Gibbs free energy of one hydrogen bond.

β9–C terminus segment is involved in the unfolding at Transition1, it is likely that the unresolved intermediate state in Transition 1 is similar to the equilibrium state of OspA[27–163]. The $\Delta H_{vH}/\Delta H_{cal}$ ratio for Transition2 is very close to unity, indicating that the observed process is a cooperative two-state transition. Thus, we can speculate the following three-step denaturing mechanism of OspA as shown in Figure 6. In the first step, β12–C terminus unfolds leaving the β9–β11 strands less stable than that in the native state. The second step is unfolding of these unstable β-strands. In the full-length protein, the first and second transitions are not resolved as separate DSC peaks. The last step is unfolding of N terminus–β8. The unfolding reaction of the N-terminal fragment (OspA[27–163]) corresponds to the second and last steps in this scheme. Our recent data from native-state amide H–^{2}H exchange experiments support this dissection into β9–β11 and β12–C terminus (S. Yan, S.D. Kennedy & S. K., unpublished results).

Contributions of various interactions to the thermodynamic parameters

To find out how the β-sheet and other structural features such as abundant polar side-chains contribute to the stability of OspA, we tried to decompose the thermodynamic parameters into contributions of hydration, van der Waals interactions, and hydrogen bonding.[29,30] All the enthalpic terms obtained according to equations (11)–(15) are given in Table 5. We obtained the enthalpy of the internal hydrogen bond (Δh^{HB}) by subtracting hydration and van der Waals interactions from the experimentally obtained enthalpy (equation (11)). Thus, Δh^{HB} includes the hydrogen bond and other polar interactions such as salt-bridges. We have found that Δh^{HB} of OspA (20 kcal mol^{-1}) is strikingly higher than that already reported. Δh^{HB} values between 6 and 12 kcal mol^{-1} have been reported for other proteins, with a tendency for higher content of α-helix showing lower enthalpy.[12] At 25 °C, it is 12 kcal mol^{-1} for an all-β protein, interleukin 1β, while it is only 6 kcal mol^{-1} for an all-α protein, myoglobin. This can be interpreted by the fact that the average length of a hydrogen bond is shorter for a β-sheet compared to that for an α-helix, resulting in higher enthalpy for the β-sheet. The strikingly large Δh^{HB} found for OspA may be because polar interaction in OspA, such as attractions between positive (e.g. Lys) and negative (e.g. Glu) charges, are abundant in OspA in addition to the hydrogen bonds in the β-sheet. Indeed, we found 26 potential ion pairs (charged groups of opposite sign located within 5 Å) among 85 charged residues in the OspA crystal structure.

From the entropies of hydration and the experimental entropies, we estimated the conformational entropy change (Table 5). It has been reported that the entropy of freezing one bond is in the range of 2–4.5 cal mol^{-1} K^{-1},[31,32] or about 20 cal mol^{-1} K^{-1}-residue^{-1} for residues with an average of five rotatable bonds. Generally, about 60–70% of all atoms are buried in a native protein,[33] giving an average value of 13 cal mol^{-1} K^{-1}residue^{-1}. OspA (67% burial) gave higher values, 19.5 cal mol^{-1} K^{-1}residue^{-1} (Table 5), suggesting that abundant long side-chains such as Lys are contributing to the higher conformational entropy change. Rigidity of these residues in the native structure of OspA due to ionic and/or hydrophobic interactions may be one of the sources of the large entropy change, which compensates partially for the large enthalpy change.

The Gibbs free energy can be calculated from enthalpy and entropy, and is given in Table 5. It is particularly important to estimate the free energy of a hydrogen bond, Δg_{hyd}^{HB}, which is a sum of the

enthalpy of the internal hydrogen bond (Δh^{HB}) and the free energy of hydration of polar groups (ΔG^{HB}_{hyd}) divided by the number of residues. The resulting values (4.4–4.6 kcal mol^{-1}; Table 5) are significantly larger than those reported for other proteins (2.5 kcal mol^{-1} for interleukin 1β and 1.1 kcal mol^{-1} for myoglobin).[12] This is presumably because there are many polar interactions that contribute the free energy existing in OspA other than hydrogen bonds in the β-sheet.

In conclusion, the stability of OspA is maintained by the large positive enthalpic contribution of hydrogen bonding and other polar interactions that overcome the large negative contribution from conformational entropy. Among other enthalpic factors, ΔH^{vdw}, which is fairly high compared to that of other proteins possibly due to the high ΔASA of non-polar parts has some additional stabilizing effects. All of these are caused by the unique structure of OspA with high content of β-sheet and polar residues with long hydrophobic methylene groups. This is a clear demonstration that the stability of a protein can be maintained to a similar extent to that of other proteins by utilizing quite different amino acid composition and the β-sheet structure. We have demonstrated that comprehensive analysis of thermal unfolding can serve as a powerful tool to find out the relationship between the structure and thermodynamics of proteins.

Materials and Methods

Sample preparation

OspA (OspA, residues 18–273) was expressed in *Escherichia coli* and purified as described.[34] The molecular mass of OspA is 27623, and its extinction coefficient at 280 nm has been determined to be 10.59 mM^{-1} cm^{-1}. OspA[27–163] was prepared as described by Huang *et al*.[26] The molecular mass of OspA[27–163] is 15252, and its extinction coefficient at 280 nm is 2.90 mM^{-1} cm^{-1}.

Differential scanning calorimetry

Calorimetric measurements were made with a Nano-DSC instrument (CSC, Utah) over a temperature range from 0 °C to 95 °C. All experiments were performed under an excess pressure of 2.5 atm. The protein solution was prepared by buffer exchange, and centrifuged for 20 minutes at 15,000 rpm (??? rotor) before DSC measurements. The concentration of the protein was 1.0–2.5 mg ml^{-1}, in 10 mM sodium phosphate buffer (pH 6) containing NaCl at concentrations between 50 and 750 mM, or in 10 mM glycine–HCl buffer containing 50 mM NaCl at acidic pH. Data taken with a scanning rate of 0.5 deg. C min^{-1} and 1.0 deg. C min^{-1} were nearly identical (data not shown). Thus, a scanning rate of 1.0 deg. C min^{-1} was employed for further measurements. The reversibility of denaturation reaction was checked by performing a second scanning of samples immediately after cooling from the first scan. The trace of the second scanning showed more than 80% agreement with that of the first scan. Analysis of the DSC data was carried out by use of a program developed in our laboratory.[35] Although the program can handle more complex systems, including dissociation and/or association processes, we set all the transitions, either two-state between N and D or three-state among N, I, and D, without such processes present in curve-fitting, since no concentration-dependence was detected experimentally.

Circular dichroism

Circular dichroism (CD) spectra in the near-UV and far-UV region of OspA were collected on a Jasco J720 spectropolarimeter (Tokyo, Japan) or an AVIV model 202 (Lakewood, NJ). The protein concentration was 1.39 mg ml^{-1} for the near-UV measurement and 0.186 mg ml^{-1} for the far-UV measurement. The solution was prepared by buffer exchange to 10 mM sodium phosphate buffer (pH 6) containing 50 mM NaCl, and centrifuged for ten minutes at 15,000 rpm (??? rotor). For CD measurements in the near-UV region, the temperature of the solution was changed with a step of 5 deg. C, with a time interval of five minutes over a temperature range from 25 °C to 40 °C and 75 °C to 90 °C, a step of 2 deg. C with a time interval of two minutes over a temperature range from 40 °C to 44 °C and 71 °C to 75 °C, and a step of 1 deg. C with a time interval of one minute over a temperature range from 44 °C to 71 °C. For CD measurements in the far-UV region, the temperature of the solution was changed with a step of 5 deg. C with a time interval of five minutes over a temperature range from 25 °C to 40 °C, a step of 2 deg. C with a time interval of two minutes over a temperature range from 40 °C to 44 °C and 78 °C to 80 °C, and a step of 1 deg. C with a time interval of 1 min over a temperature range from 45 °C to 78 °C. The melting curve of OspA[27–163] at 230 nm was collected. OspA[27–163] was prepared by dissolving in the same buffer as that used in OspA measurement at concentrations of 0.148 mg ml^{-1}. The temperature of the sample was controlled at a heating rate of 50 deg. C hour^{-1}.

The experimentally observed ellipticity (θ) is assumed to be proportional to the concentration of each species. The concentration can be defined by the equilibrium constant, K, according to the two-state mechanism:

$$N \rightleftharpoons D \quad K_1 = [D]/[N] \tag{8}$$

or the three-state mechanism:

$$N \rightleftharpoons I \rightleftharpoons D \qquad K_2 = [I]/[N],\ K_3 = [D]/[I] \tag{9}$$

where N, I and D represent the native, intermediate, and denatured states, respectively. Temperature-dependence is determined by the van't Hoff equation:

$$K_i = A_i \exp(-\Delta H_{vHi}/RT) \tag{10}$$

where i is 1, 2, or 3, ΔH_{vH} is the van't Hoff enthalpy, A is a constant, R is the gas constant, and T is the absolute temperature. Here, we assumed that ΔH_{vH} is temperature-independent. These parameters were obtained by curve-fitting the experimental data to these equations. The denaturation temperature, t_m, where the reaction is half-completed, was calculated from ΔH_{vH} and A.

Decomposition of thermodynamic parameters into different interactions

The experimentally measured enthalpy, ΔH_{cal} can be represented as the sum of the hydration enthalpies of

polar, $\Delta H_{\mathrm{pol}}^{\mathrm{hyd}}$, and non-polar groups, $\Delta H_{\mathrm{npl}}^{\mathrm{hyd}}$, the enthalpy of van der Waals interactions between non-polar groups, ΔH^{vdw}, and the enthalpy of internal hydrogen bonding between polar groups, ΔH^{HB} :

$$\Delta H_{\mathrm{cal}} = \Delta H_{\mathrm{pol}}^{\mathrm{hyd}} + \Delta H_{\mathrm{npl}}^{\mathrm{hyd}} + \Delta H^{\mathrm{vdw}} + \Delta H^{\mathrm{HB}} \quad (11)$$

Each of these contributions is related to structural features of the protein as

$$\Delta H_{\mathrm{npl}}^{\mathrm{hyd}}(T) = \sum_i \Delta \mathrm{ASA}_{\mathrm{npl},i} \Delta \hat{H}_{\mathrm{npl},i}^{\mathrm{hyd}}(t) \quad (12)$$

$$\Delta H_{\mathrm{pol}}^{\mathrm{hyd}}(T) = \sum_k \Delta \mathrm{ASA}_{\mathrm{pol},k} \Delta \hat{H}_{\mathrm{pol},k}^{\mathrm{hyd}}(t) \quad (13)$$

$$\Delta H^{\mathrm{vdw}} = \Delta \hat{H}_{\mathrm{arm}}^{\mathrm{vdw}} \Delta \mathrm{ASA}_{\mathrm{arm}} + \Delta \hat{H}_{\mathrm{alp}}^{\mathrm{vdw}} \Delta \mathrm{ASA}_{\mathrm{alp}} \quad (14)$$

$$\Delta H^{\mathrm{HB}} = N_{\mathrm{HB}} \Delta h^{\mathrm{HB}} \quad (15)$$

where $\Delta \hat{H}_i^{\mathrm{hyd}}$ is the reduced enthalpy of hydration of an accessible surface area and $\Delta \hat{H}^{\mathrm{vdw}}$ is the reduced enthalpy of van der Waals interaction between aliphatic or aromatic residues.[2] N_{HB} is the number of hydrogen bonds and Δh^{HB} is the enthalpy of an internal hydrogen bond in a protein.

The entropy of hydration of non-polar and polar groups of the protein can be represented as follows:

$$\Delta S^{\mathrm{ex}} = \Delta S_{\mathrm{pol}}^{\mathrm{hyd}} + \Delta S_{\mathrm{npl}}^{\mathrm{hyd}} + \Delta S^{\mathrm{cnf}} \quad (16)$$

where $\Delta S_{\mathrm{pol}}^{\mathrm{hyd}}$ and $\Delta S_{\mathrm{npl}}^{\mathrm{hyd}}$ are the entropies of hydration of non-polar and polar groups, respectively, and ΔS^{cnf} is the configurational entropy of disruption of hydrogen bonds and unpacking side-chain groups. The hydration terms are assumed to be proportional to the change in accessible surface area:

$$\Delta S_{\mathrm{npl}}^{\mathrm{hyd}} = \sum_i \Delta \mathrm{ASA}_{\mathrm{npl},i} \Delta \hat{S}_{\mathrm{npl},i}^{\mathrm{hyd}} \quad (17)$$

$$\Delta S_{\mathrm{pol}}^{\mathrm{hyd}} = \sum_k \Delta \mathrm{ASA}_{\mathrm{pol},k} \Delta \hat{S}_{\mathrm{pol},k}^{\mathrm{hyd}} \quad (18)$$

where $\Delta \hat{S}_i^{\mathrm{hyd}}$ are the hydration entropies of a given type of surface area on a per square angstrom basis.[30]

Acknowledgements

We thank S. Yan for critical reading of the manuscript, K. Akasaka for use of the DSC equipment, and Shimadzu cooperation for use of the CD equipment (AVIV model 202). This work is supported, in part, by a Grant-in-Aid for Scientific Research from the Ministry of Education, Science, Sports, and Culture of Japan (to A.T.) and by NIH grant R01-GM57215 (to S.K.).

References

1. Privalov, P. L. (1979). Stability of proteins small globular proteins. *Advan. Protein Chem.* **33**, 167–241.
2. Makhatadze, G. I. & Privalov, P. L. (1995). Energetics of protein structure. *Advan. Protein Chem.* **47**, 307–425.
3. Pal, U., de Silva, A. M., Montgomery, R. R., Fish, D., Anguita, J., Anderson, J. F. *et al.* (2000). Attachment of *Borrelia burgdorferi* within *Ixodes scapularis* mediated by outer surface protein A. *J. Clin. Invest.* **106**, 561–569.
4. Pal, U., Montgomery, R. R., Lusitani, D., Voet, P., Weynants, V., Malawista, S. E. *et al.* (2001). Inhibition of *Borrelia burgdorferi*-tick interactions *in vivo* by outer surface protein A antibody. *J. Immunol.* **166**, 7398–7403.
5. Li, H., Dunn, J. J., Luft, B. J. & Lawson, C. L. (1997). Crystal structure of Lyme disease antigen outer surface protein A complexed with an Fab. *Proc. Natl Acad. Sci. USA*, **94**, 3584–3589.
6. Pham, T. N. & Koide, S. (1998). NMR studies of *Borrelia burgdorferi* OspA, a 28 kDa protein containing a single-layer β-sheet. *J. Biomol. NMR*, **11**, 407–417.
7. Bu, Z., Koide, S. & Engelman, D. M. (1998). A solution SAXS study of *Borrelia burgdorferi* OspA, a protein containing a single-layer β-sheet. *Protein Sci.* **7**, 2681–2683.
8. Pham, T. N., Koide, A. & Koide, S. (1998). A stable single-layer β-sheet without a hydrophobic core. *Nature Struct. Biol.* **5**, 115–119.
9. Koide, S., Huang, X., Link, K., Koide, A., Bu, Z. & Engelman, D. M. (2000). Design of single-layer β-sheets without a hydrophobic core. *Nature*, **403**, 456–460.
10. Schenck, H. L. & Gellman, S. H. (1998). Use of a designed triple-stranded antiparallel β-sheet to probe β-sheet cooperativity in aqueous solution. *J. Am. Chem. Soc.* **120**, 4869–4870.
11. Kortemme, E., Ramirez-Alvarado, M. & Serrano, L. (1998). Design of a 20-amino acid, three-stranded β-sheet protein. *Science*, **281**, 253–256.
12. Makhatadze, G. I., Clore, G. M., Granenborn, A. M. & Privalov, P. L. (1994). Thermodynamics of unfolding of the all β-sheet protein interleukin-1β. *Biochemistry*, **33**, 9327–9332.
13. Viguera, A. R., Martinez, J. C., Filimonov, V. V., Mateo, P. L. & Serrano, L. (1994). Thermodynamic and kinetic analysis of the SH3 domain of spectrin shows a two-state folding transition. *Biochemistry*, **33**, 2142–2150.
14. Samuel, D., Krishnaswamy, T., Kummer, S., Srimathi, T., Heieh, H. & Yu, C. (2000). Identification and characterization of an equilibrium intermediate in the unfolding pathway of an all β-barrel protein. *J. Biol. Chem.* **275**, 34968–34975.
15. Perez, J., Vachette, P., Russo, D., Desmadril, M. & Durand, D. (2001). Heat-induced unfolding of neocarzinostatin, a small all-β protein investigated by small-angle X-ray scattering. *J. Mol. Biol.* **308**, 721–743.
16. Regan, L. (1994). Born to be beta. *Curr. Biol.* **4**, 656–658.
17. Honda, S., Kobayashi, N. & Munekata, E. (2000). Thermodynamics of a β-hairpin structure: evidence for cooperative formation of folding nucleus. *J. Mol. Biol.* **295**, 269–278.
18. Macias, M. J., Gervais, V., Civera, C. & Oschkinat, H. (2000). Structural analysis of WW domains and design of a WW prototype. *Nature Struct. Biol.* **7**, 375–379.
19. Koide, S., Bu, Z., Rasal, D., Pham, T. N., Nakagawa, T., Tamura, A. & Engelman, D. M. (1999). Multistep denaturation of *Borrelia burgdorferi* OspA, a protein containing a single-layer β-sheet. *Biochemistry*, **38**, 4757–4767.

20. Tamura, A., Kojima, S., Miura, K. & Sturtevant, J. M. (1994). Effect of an intersubunit disulfide bond on the stability of *Streptomyces* subtilisin inhibitor. *Biochemistry*, **33**, 14512–14520.
21. Makhatadze, G. I. & Thomas, S. T. (1998). Anion binding to the ubiquitin molecule. *Protein Sci.* **7**, 689–697.
22. Wassenberg, D. & Jaenicke, R. (1999). Thermodynamics of the unfolding of the cold-shock protein from *Thermotoga maritima*. *J. Mol. Biol.* **289**, 187–193.
23. Izatt, R. M. & Christensen, J. J. (1970). Heat of proton ionization, p*K*, and related thermodynamic quantities. In *Handbook of Biochemistry, Selected Data for Molecular Biology* (Sober, H. A., ed.), CRC Press, Cleveland, OH.
24. Fasman, G. D. (1996). *Circular Dichroism and the Conformational Analysis of Biomolecules*, Plenum Press, New York.
25. France, L. L., Kieleczawa, J., Dunn, J. J., Hind, G. & Sutherland, J. C. (1992). Structural analysis of an outer surface protein from the Lyme disease spirochete, *Borrelia burgdorferi*, using circular dichroism and fluorescence spectroscopy. *Biochim. Biophys. Acta*, **1120**, 59–68.
26. Huang, X., Nakagawa, T., Tamura, A., Link, K., Koide, A. & Koide, S. (2001). Formation of the single-layer β-sheet of *Borrelia burgdorferi* OspA in the absence of the C-terminal capping globular domain. *J. Mol. Biol.* **308**, 367–375.
27. Spolar, R. S., Livingstone, J. R. & Record, J. M. T. (1992). Use of liquid hydrocarbon and amide transfer data to estimate contributions to thermodynamic function of protein folding from the removal of nonpolar and polar surface from water. *Biochemistry*, **31**, 3947–3955.
28. Yutani, K., Ogasahara, K. & Kuwajima, K. (1992). Absence of the thermal transition in Apo-α-lactalbumin in the molten globule state. *J. Mol. Biol.* **228**, 347–350.
29. Privalov, P. L. & Makhatadze, G. I. (1993). Contribution of hydration to protein folding thermodynamics. *J. Mol. Biol.* **232**, 660–679.
30. Makhatadze, G. I. & Privalov, P. I. (1993). Contribution of hydration to the protein folding thermodynamics. I. The enthalpy of hydration. *J. Mol. Biol.* **232**, 639–659.
31. Novotony, J., Bruccoleri, R. E. & Saul, F. A. (1989). On the attribution of binding energy in antigen–antibody complex McPC 603, D1.3, and HyHEL-5. *Biochemistry*, **28**, 4735–4749.
32. Page, M. L. & Jencks, W. P. (1971). Entropic contributions to rate accelerations in enzymic and intramolecular reactions and the chelate effect. *Proc. Natl Acad. Sci. USA*, **68**, 1678–1683.
33. Miller, S., Janin, J., Lesl, A. M. & Chothia, C. (1987). Interior and surface of monomeric proteins. *J. Mol. Biol.* **196**, 641–656.
34. Dunn, J. J., Lade, B. N. & Barbour, A. G. (1990). Outer surface protein A (OspA) from the Lyme disease spirochete, *Borrelia burgdorferi*: high level expression and purification of a soluble recombinant form of OspA. *Protein Express. Purif.* **1**, 159–168.
35. Tamura, A. & Sturtevant, J. M. (1995). A thermodynamic study of mutant forms of *Streptomyces* subtilisin inhibitor. 1. Hydrophobic replacements at the position of Met103. *J. Mol. Biol.* **249**, 625–635.
36. Lesser, G. J. & Rose, G. D. (1990). Hydorophobicity of amino acid subgroups in proteins. *Proteins: Struct. Funct. Genet.* **8**, 6–13.

Edited by P. Wright

(Received 20 May 2002; received in revised form 3 September 2002; accepted 4 September 2002)